

## Supporting Information Available

### **Bio-synthesis Participated Mechanism of Mesoporous LiFePO<sub>4</sub>/C Nanocomposite Microspheres for Lithium Ion Battery**

Xudong Zhang,<sup>a</sup> Wen He,<sup>\*a</sup> Yuanzheng Yue,<sup>ab</sup> Ruiming Wang,<sup>c</sup> Jianxing Shen,<sup>a</sup> Shujiang Liu,<sup>a</sup> Jingyun Ma,<sup>a</sup> Mei Li<sup>a</sup> and Fengxiu Xu<sup>a</sup>

\*Corresponding author, Prof. Wen He: hewen1960@126.com

<sup>a</sup> Shandong provincial key laboratory of processing and testing technology of glass and functional ceramics, Key Laboratory of Amorphous and Polycrystalline Materials, Department of Materials Science and Engineering, Shandong Polytechnic University, Jinan, China. Fax: +86 531 89631518; Tel: +86 531 89631018;

E-mail: hewen@126.com

<sup>b</sup> Section of chemistry, Aalborg University, Aalborg, Denmark. Fax: +45 96350558; Tel: +45 96358522; E-mail: yy@bio.aau.dk

<sup>c</sup> Shandong key laboratory of Fermentation Engineering, Shandong Polytechnic University, Jinan, China. Tel: +86 531 89631076; E-mail: ruiming3k@163.com

### **Submitted to Journal of Materials Chemistry**

**S1: Particle size distribution analysis**

**S2: Performance analysis of synthesized materials**

**S3: Cycle stability at high current ratio and Cyclic voltammogram for the**

**MP-LFP/C-NC-MS cathode**

### S1: Particle size distribution analysis

The particle size distribution of the MP-LFP/C-NC-MS sample, as shown in **Figure S1**, was evaluated by a laser diffraction particle size analyzer. The porous microsphere distribution was essentially a log-normal distribution. The mean size of MP-LFP/C-NC-MS was 4.76 $\mu\text{m}$ , and agrees with that estimated from the SEM observation.

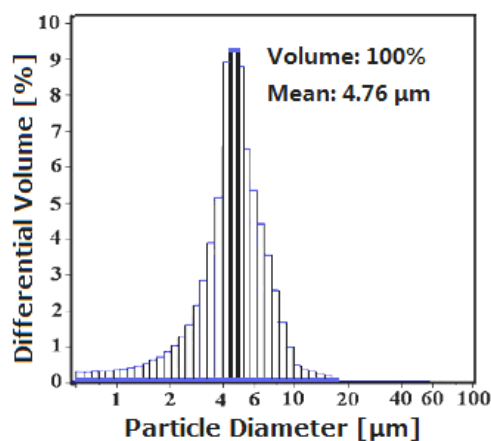


**Figure S1.** Particle size distribution of the MP-LFP/C-NC-MS sample synthesized by using genetic control and biomolecular self-assembly method and calcined at 600 °C for 6 h.

### S2: Performance analysis of synthesized materials

**Table S1** shows the specific surface area and the tap density of the samples with various carbon amounts. The specific areas of the samples rapidly increase with increasing of the carbon amount, but the sample containing 12.9% carbon exhibits the highest tap density of 1.74 g cm<sup>-3</sup>. The specific surface area and the tap density of MP-LFP/C-NC-MS are observably higher than that of the pure LiFePO<sub>4</sub> sample obtained without using yeast cell template. The high specific surface area is mainly attributed to the porous network structure of amorphous carbon, and the high tap density is due to the nanocomposite microsphere structure. With continuous increase in carbon amount, the tap density decreases due to the accumulation of the excessive carbon.

**Table S1.** Specific Surface Area and Tap Density of Samples Calcined at 600 °C for 6 h with Various Carbon Amounts

Samples	Carbon Amounts (%)					
	0	3.24	6.89	12.90	16.87	19.13
Specific Surface Areas ( $\text{m}^2 \text{g}^{-1}$ )	55.1	120.3	165.2	203.0	218.1	238.5
Tap Density ( $\text{g cm}^{-3}$ )	1.12	1.58	1.55	1.74	1.69	1.51

**Table S2.** Specific Surface Area and Electrical Conductivity of Samples Calcined at Different Temperatures for 6 h.

Samples	Calcining temperatures (°C)				
	120	400	500	600	700
Specific Surface Areas ( $\text{m}^2 \text{g}^{-1}$ )	97.2	146.9	157.3	203.0	87.6
Electrical conductivity ( $\text{S cm}^{-1}$ )	$7.1 \times 10^{-6}$	$1.9 \times 10^{-4}$	$3.7 \times 10^{-3}$	$2.5 \times 10^{-2}$	$3.9 \times 10^{-4}$

**Table S2** displays the specific surface area and the electrical conductivity of the samples calcined at different temperatures for 6 h. The boicarbon obtained by heating yeast cells plays an important role in the enhancement of specific surface area and electrical conductivity. With an increase in calcination temperature, the electrical conductivity of the samples drastically increases from  $7.1 \times 10^{-6}$  to  $2.5 \times 10^{-2}$  S/cm. But when the calcination temperature is increased to 700 °C, the electrical conductivity drops to  $3.9 \times 10^{-4}$  S/cm because of the loss of mesoporous structure.

**S3: Cycle stability at high current ratio and Cyclic voltammogram for the MP-LFP/C-NC-MS cathode**

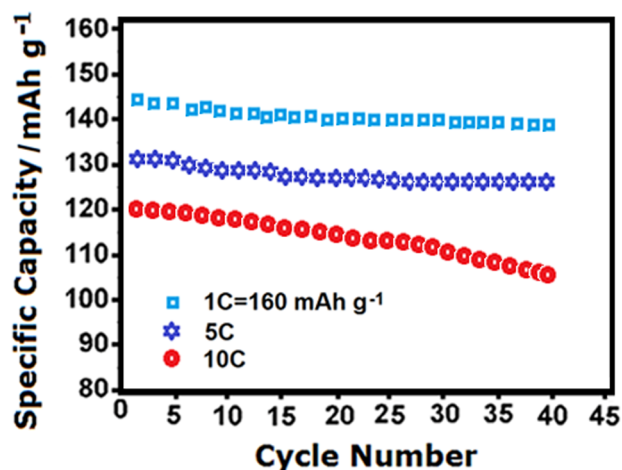


**Figure S2.** Cycle stabilities of the MP-LFP/C-NC-MS cathode at high current ratio at room temperature in the voltage of 2.0–4.3V.

The cycle stability of the MP-LFP/C-NC-MS electrodes calcined at 600 °C at high current ratio was investigated in terms of cycle stability during constant current (CC) cycling tests. All electrodes were subjected to 40 cycles at different current rates at room temperature in the voltage of 2.0–4.3V. As shown in Figure S2, all electrodes displayed excellent cycling stability. The MP-LFP/C-NC-MS electrode delivers the highest initial discharge capacities of 143 mA·h g<sup>-1</sup> at a current rate of 1 C, and maintains the most impressive discharge capacity of 140 (97.9% of its initial value) after 40 cycles. This cathode displayed a capacity about 122 mAhg<sup>-1</sup> at a current rate of 10 C, and maintains the discharge capacity of 106 (86.9% of its initial value) after 40 cycles. This could be attributed to the appropriate morphology of microspheres, nanocomposite structure of the LiFePO<sub>4</sub>/C particles, high electrical conductivity and high tap density. These show that the

cycle number is larger, our method can be better manifested the improvement of the already commercialized cathode material.

The CV analysis is widely used to study the oxidation/reduction and/or phase transformation processes in electrode reactions. **Figure S3** shows the cyclic voltammogram of the MP-LFP/C-NC-MS cathode. The cathode exhibited sharp oxidation (3.5 V) and reduction (3.3 V) peaks, and this is consistent with a two-phase reaction at about 3.4 V versus  $\text{Li}/\text{Li}^+$ . No other peaks are observed, evidencing the absence of electroactive iron impurities. The well-defined peaks, the symmetrical form of the CV plots, and its good reproducibility, confirm the outstanding reversibility of the lithium extraction/insertion reactions in this sample. This result is consistent with the cycle stability performance of the materials as demonstrated in Figure 5b.

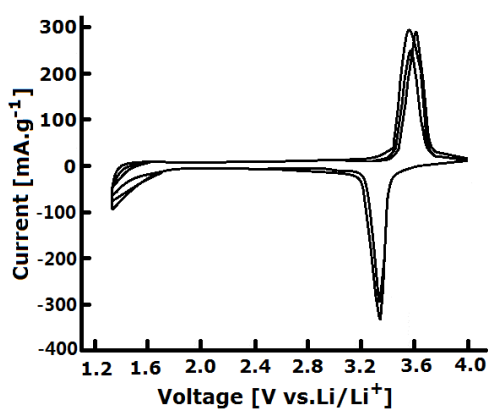


**Figure S3.** Cyclic voltammogram of the MP-LFP/C-NC-MS cathode at  $0.1 \text{ mV s}^{-1}$  (three cycles).